

## **INTEGRATED INTERPRETATION OF GEOPHYSICAL EXPLORATION DATA FOR DETECTING RESERVOIR-TYPE ANOMALIES**

R. G. BERZIN, E. A. KOZLOV, O. A. POTAPOV, V. S. PAVLUSHIN,  
Y. A. TARASOV, S. S. CHAMO\*

The efficiency of integrating geophysical methods for reservoir delineation and location of water lenses therein is demonstrated with reference to a hydrocarbon deposit in south-west Turkmenia. Although seismics is the most informative method, high-accuracy gravity and geoelectric prospecting yield important additional geophysical data thereby increasing the reliability of locating geological inhomogeneities, zones of lithofacies changes in reservoirs, and gas-water and oil-water interfaces.

**d: oil and gas fields, oil-gas interface, oil-water interface, seismic methods, magnetotelluric methods, transient methods, statistical analysis**

### **1. Introduction**

As more and more complicated problems must be solved associated with the exploration and prospecting of deep-seated objects containing gas and oil, the identification of structural traps differing from anticlinal ones, gas—water—oil interfaces and zones of lithofacies changes in reservoirs, the necessity arises to integrate geophysical methods. Experience has recently been gained in the integrated use of geophysical methods enabling, in numerous cases, much more accurate and reliable identification of the objects being sought for and allowing problem solution at a higher geological and economic level.

This paper deals with integration as a method for the more reliable identification and tracing of the gas—water—oil interfaces of a large condensed gas field of unusual structure in south-east Turkmenia.

### **2. Description of region**

As shown by the data of geophysical – primarily seismic – investigations and deep drillings carried out within the examined region, its structure is represented by two large dissimilar tectonic elements linked together: the deep-seated Murgab depression in the north and a zone of large swell-like structural

\* NPO Neftegeofizika, 103062 Moscow, Chernyshevskogo 22, USSR  
Paper presented at the 28th International Geophysical Symposium, Balatonszemes, Hungary,  
28 September — 1 October, 1983

height forming the Badkhyz—Karabil—Maimanin elevated zone in the south. On closer examination, three zones can be distinguished within it: the top of the swell-like uplift in the south, monoclinal north-dipping beds in the centre, and an extensive terrace-like zone in the north.

The top of the swell-like uplift has a particularly complex tectonic pattern, as there is a series of local small-amplitude heights and zones of tectonic dislocations.

The zone of monoclinal north-dipping beds has a much simpler tectonic pattern. Judging by the results of the refraction correlation method (RCM), a large deep-seated fault zone is enclosed within it thus complicating the structure of the crystalline basement and the deeper layers of the earth's crust.

The terrace-like zone in the north is nearly flat-bedded with local small-amplitude heights not very large in size.

The gas field itself has a most unusual structure due to two peculiarities of its spatial and areal situation. Firstly, the field is restricted to the Hauerivian sandstones and is very extended. Within its boundaries the depth of the pay zone changes from 2800 to 3600 m in a monoclinal manner, i.e. its localization is influenced somewhat by structural factors. Secondly, an extensive lens has been detected within the field that is characterized by higher water content and noticeable decrease or lack of gas-saturation.

### **3. Investigation**

It may be expected that direct detection within such fields of unusual structure and considerable size (cross-sectional width is over 55—60 km) will be very difficult and not highly effective at the initial stage because of numerous factors, the principal ones being:

- a) Extremely unfavourable seismogeological conditions on the surface and at lower depths (twice or three-times layered low velocity zone (LVZ) with a thickness ranging from 10—15 to 200 m) giving a low signal-to-noise ratio.
- b) Complex tectonic pattern of the examined irregular object and specific structural conditions of its spatial localization (crowns, monoclinal dips, deep-seated zones with subhorizontal altitudes of bedding, etc.).
- c) High probability of the presence of other irregularities within the section of such an extended field, associated both with water lenses (places of higher water content) and with lithofacies changes, fault zones, unconformities, pinching out, local changes in surface conditions, etc.
- d) Lack of experience in prospecting giant fields of this kind.

The above peculiarities pointed to the need for high-facility geophysical investigations using advanced digital equipment to refine the structural details and to identify and trace within the area the contours of irregularities associated with the gas field and high water content lenses.

Geophysical investigations were performed in two steps. In the first step

all available seismic data (5000 km CDP profiles) were processed by a fast-analysing program to yield integral characteristics.

Characteristic shapes of plots for absorption parameters  $\beta$  and  $\delta$  (local, not too long high-gradient zones) together with higher  $R(t)$  values of the autocorrelation function helped to provide preliminary identification and trace a series of anomalous zones presumably associated with gas—water interfaces in the western, northern and southern parts of the area (*Fig. 1*).

Lower absorption parameters in the central part of the area indicated a transition zone with possibly smaller gas content and with a high gradient zone inside it. Unambiguous interpretation of these data, however, did not seem possible without more reliable data of deep drillings and integrated geophysical methods including digital seismic prospecting. Therefore integrated field studies were carried out simultaneously, including CRP prospecting that ensures 24-fold coverage, high-facility areal gravity prospecting and modified methods of electric prospecting — magnetotelluric sounding (MT) and transient electromagnetic sounding (TEM).

The results of all these field studies were processed by computer using a standard graph and a set of programs for special-purpose data analysis.

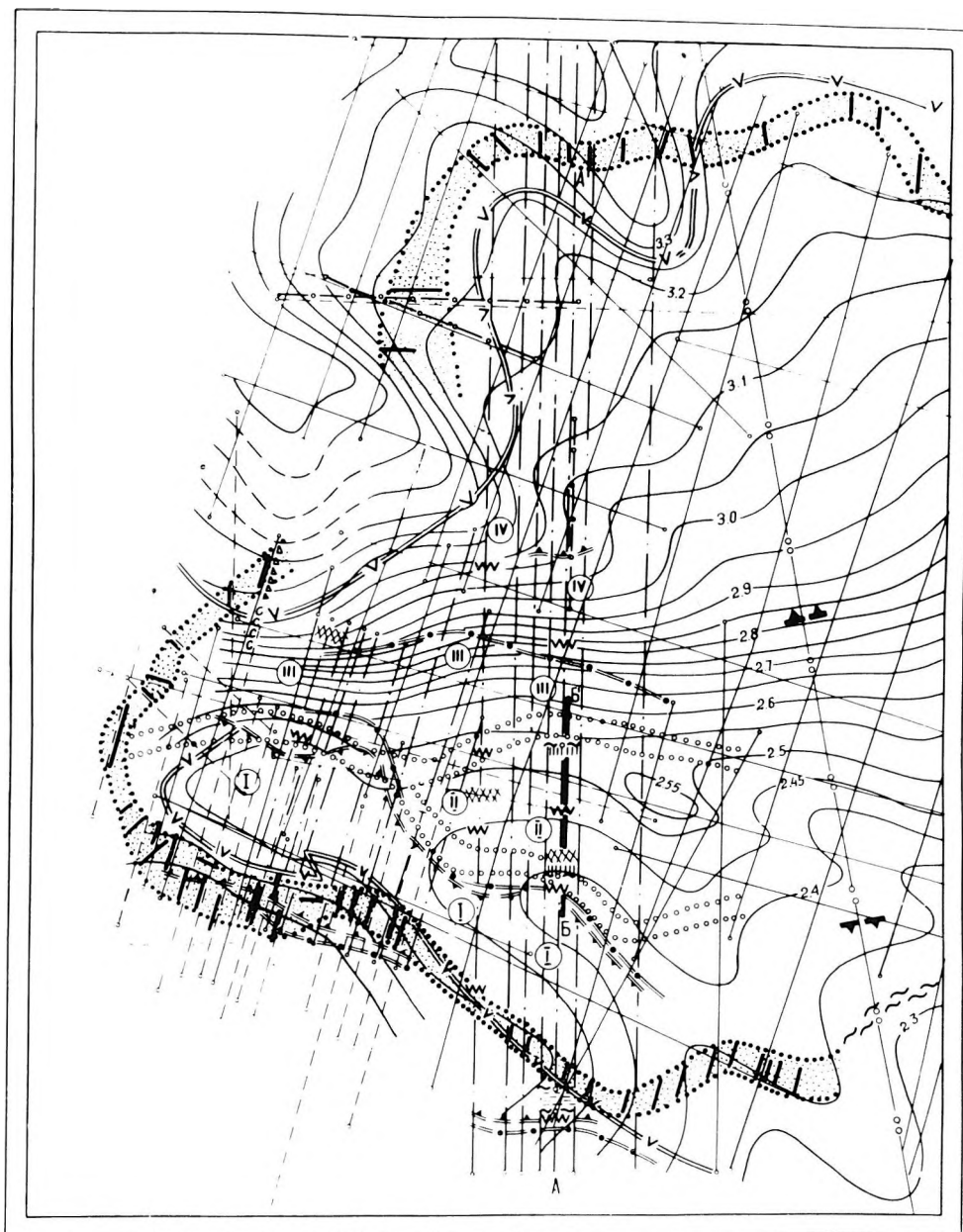
#### 4. Interpretation

The results are reported citing as an example one of the seismic sections crossing the whole gas field and the contained water lens in the near N—S direction.

If one analyses the basic characteristics of the wave field (*Fig. 2*) it can be seen that a series of key or characteristic seismic horizons can be singled out within the interval of interest on the geological section. Firstly there is a well-defined key reflecting horizon restricted to Bukhara limestones of the Lower Palaeogene, whose signal is recorded within 1.0—1.1 s. Then follows a carbonate bed dating back to the Lower Aptian—Upper Barremian ( $t_0 = 1.8 - 1.9$  s) and a terrigenous carbonate layer of the Hauterivian ( $t_0 = 1.85 - 2.0$  s). In addition, a number of characteristic horizons were recorded on the section, confined to the Middle Palaeogene ( $t_0 = 0.7 - 0.9$  s) and Upper Cretaceous:  $K_3^S(t \approx 1.35 - 1.45$  s),  $K_3^I(t \approx 1.5 - 1.6$  s).

The pay-zone is confined to Hauterivian sandstones, which gives the Lower Cretaceous sand-and-carbonate complex and its geophysical characteristics great importance.

The detailed velocity analysis was made in the time interval of 1.0—2.4 s. Horizontal spectra give information on velocity characteristics  $V_{CRP}$  for four reflecting horizons: Bukhara limestones of the Lower Palaeogene, and sand-carbonate beds of the Barremian, Hauterivian and Upper Jurassic stages. Layer velocities  $V_l$  are characterizing the change of the properties in section intervals bounded by the indicated horizons.



- A row of numbered boxes (1-20) containing symbols for a dot-to-dot puzzle. The symbols include: 1. A horizontal line with a circle at each end. 2. A horizontal line with a triangle at each end. 3. A horizontal line with a square at each end. 4. A horizontal line with a diamond at each end. 5. A horizontal line with a circle at each end. 6. A horizontal line with a triangle at each end. 7. A horizontal line with a square at each end. 8. A horizontal line with a diamond at each end. 9. A horizontal line with a circle at each end. 10. A horizontal line with a triangle at each end. 11. A horizontal line with a square at each end. 12. A horizontal line with a diamond at each end. 13. A horizontal line with a circle at each end. 14. A horizontal line with a triangle at each end. 15. A horizontal line with a square at each end. 16. A horizontal line with a diamond at each end. 17. A horizontal line with a circle at each end. 18. A horizontal line with a triangle at each end. 19. A horizontal line with a square at each end. 20. A horizontal line with a diamond at each end.

*Fig. 1. Sketch map of anomalous zones in the investigated area*

1 — contours of the bottom of the Hauterivian producing layer (IV); 2 — zone of greater values of absorption parameters, presumably associated with minor dislocations surrounding the water lens; 3 — zones of large basement faults (from refraction survey); 4 — assumed tectonic dislocations (TEM data);  
 5 — reflection profiles; 6 — CDP profiles; 7 — refraction profiles; 8 — electric and gravity profiles; 9 — inner contour of gas reservoir from borehole data; 10 — band of abnormally high values of absorption parameters, presumably associated with gas–water interface; 11 — zones of high absorption parameter gradients resulting from gas–water interface irregularities; 12 — water lens; 13 — anomalous zones of seismic wave field (“flat spots”) for the Hauterivian (upper mark) and for the upper Jurassic (lower mark); 14 — abnormally high absorption zones at traveltimes greater than 2.9 s (Jurassic); 15 — boundaries of transient electromagnetic anomalies; 16 — zone of higher values of summarized longitudinal conduction and vertical increments of apparent conduction using MT data, presumably associated with the water lens; 17 — anomalous zone of MT parameters presumably associated with gas–water interface; 18 — outer contour of gas presence from gravity data; 19 — boundaries of second order gravity zones; 20 — possible contour of gas–water contact

*1. ábra. A kutatott terület anomáliáinak vázlata*

1 — az hauerivi termelő réteg aljának izohipszái (IV); 2 — valószínűleg a vizlencse körélie kisebb diszlokációknak megfelelő magas abszorpciójú zónák; 3 — az aljzat töréseinek zónája (refraktíciós mérések ből); 4 — feltételezett tektonikus diszlokációk (TEM-adatok); 5 — reflexiószelvények; 6 — CDP-szelvények; 7 — refraktíciós szelvények; 8 — elektromos és gravitációs szelvények; 9 — a gáztároló belső kontúrja, fúrási adatok alapján; 10 — valószínűleg víz–gáz határfelülettel kapcsolatos magas abszorpciójú anomáliák; 11 — feltehetőleg a gáz–víz határ egyenetlenségeivel kapcsolatos abszorpció–gradiens anomáliák; 12 — vizlencse; 13 — hauerivi (felső jel) és felső jura (alsó jel) összleteknek megfelelő szeizmikus anomáliák („flat spots”); 14 — 2.9 s-nál nagyobb menetidőknek (jura) megfelelő abszorpciósi anomáliák; 15 — TEM anomáliák határa;  
 16 — feltehetően a vizlencsével kapcsolatos MT-anomáliák: az összegzett hosszirányú vezetőképesség és a vertikális látszólagos vezetőképesség megnövekedett értékeinek zónái; 17 — feltehetően a gáz–víz határral kapcsolatos MT-anomáliák; 18 — a gáztároló külső kontúrja, gravitációs mérések ből; 19 — a másodrendű gravitációs zónák határa; 20 — gáz–víz kontaktus valószínű határa

*Рис. 1. Схематическая карта аномальных зон на площади исследований в сопоставлении с данными глубокого бурения*

1 — стратоизогипсы подошвы продуктивного горизонта (IV) готеривского яруса; 2 — зона повышенных значений параметров поглощения, предположительно связанная с мелкими нарушениями, ограничивающими водяную линзу; 3 — зоны крупных разломов в фундаменте (по КМПВ); 4 — предполагаемые тектонические нарушения (данные ЗСМ);  
 Сейсмические профили; 5 — МОВ; 6 — МОГТ; 7 — КМПВ; 8 — Электро и гравиразведочные профили; 9 — внутренний контур газоносности по геологическим данным; 10 — полоса аномально высоких значений параметров поглощения, предположительно связанные с ГВК; 11 — зоны максимальных градиентов (ЗМГ) параметров поглощения, обусловлен неоднородностями в полосе ГВК; 12 — площадь водяной линзы; 13 — участки аномальной структуры волнового сейсмического поля («плоские пятна»), характеризующего готеривский комплекс; 14 — зоны аномально высокого поглощения, выделяемые на временах более 2.9 с (юра); 15 — границы электрических аномалий ЗСМ; 16 — зона повышенных значений суммарной продольной проводимости и вертикальных приращений кажущейся проводимости по данным МТЗ, предположительно связанные с водяной линзой; 17 — аномальная зона параметров МТЗ, возможно связанные с ГВК; 18 — внешний контур нефтеносности по гравиметрическим данным; 19 — границы гравитационных зон II порядка; 20 — возможное продолжение внутреннего контура ГВК на ЮВ площади

The results derived calculating  $V_i$  values between two Neocomian horizons  $K_1 br$ — $K_1 h$  are of the greatest interest. Analysis of the  $V_i(X)$   $K_1 br$ — $K_1 h$  curve and its comparison with the geological data show that no distinct and reliable correlation exists between velocity and section irregularities. For this bed within field boundaries a zone of low  $V_i$  values turns out to be rather wide, with three local maxima within it. The most well-defined maximum is attributed to the water lens (*Fig. 2*); the nature of the other two maxima is unknown so far.

The  $V_i$  data fail to delineate clearly the gas—water interfaces as well. The  $V_i$  values tend to increase only at the southern end of the field.

Thus parameter ( $V_i$ ) can hardly be a basic detector for identification of section irregularities of interest under the given seismogeological conditions (small pay zone thickness — not exceeding 25—40 m resulting in gross errors in velocity measurements, comparable with expected anomalies of 0.5—0.6 km/s; complex tectonic pattern of field and widely varying low velocity zone thickness, etc.). The data of this analysis, however, should not be neglected when starting complex data processing, since they make the statistical data set more complete.

Dynamic characteristics of reflected waves were studied by the corrected amplitude time section (CATS) and by analysing the amplitudes and quasi-periods for each horizon using a computer program. Analysis of corrected amplitude time section data for the Neocomian horizons indicates with fair certainty a water lens characterized by clearly visible general amplitude decrease of the wave reflected from the top of the pay zone.

Amplitude decrease is particularly abrupt within loci confined to shear zones. It is also quite distinct in the time section (*Fig. 2*). Summarized, the water lens is characterized by sudden level changes over short intervals on records of the reflected wave. Structural peculiarities of dynamic characteristics of waves from the Neocomian horizons, found on corrected amplitude time sections, conform fairly well with the calculated data on quantitative amplitude characteristics. Within the water lens, for example, a reduction of 6—8 dB was obtained for intensity of the wave from the top of pay zones and a significant lengthening of quasi-periods. Distinct quasi-period lengthening was also recorded within the southern gas—water interfaces and outside the section contours.

To analyse and study the dynamic parameters of reflected waves we used the computer program package “Command” for two types of seismograms, i.e. for the standard time section and for the corrected amplitude time section. The applied time window was 100 ms with 50 ms equalization in both directions related to the interval centre-line corresponding to the time of the basic phase of the horizon being analysed. As a result, the summarized dynamic parameter ( $\Sigma$ ) for the wave from the top of the pay zone made it clear that an anomalous zone does exist within the water lens. The standard time section provided a well-recorded minimum of the parameter  $\Sigma$  within this zone, looking like a long band of negative values. The corrected amplitude time section also proved the existence of this minimum but the anomalous zone is even more recognizable by the dispersed values of the single and summarized parameters (*Fig. 3*). By the minima of parameter  $\Sigma$  the off-contour parts of the gas field can be distin-

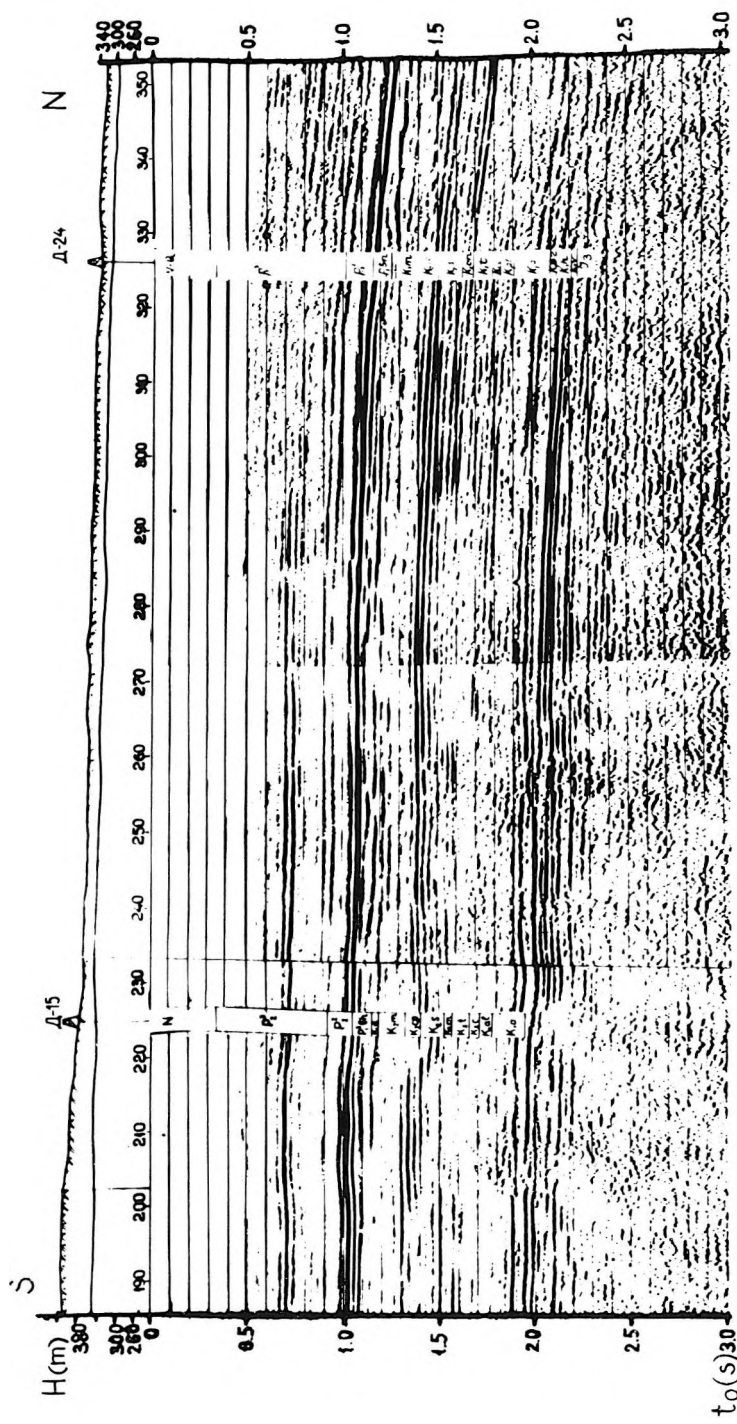
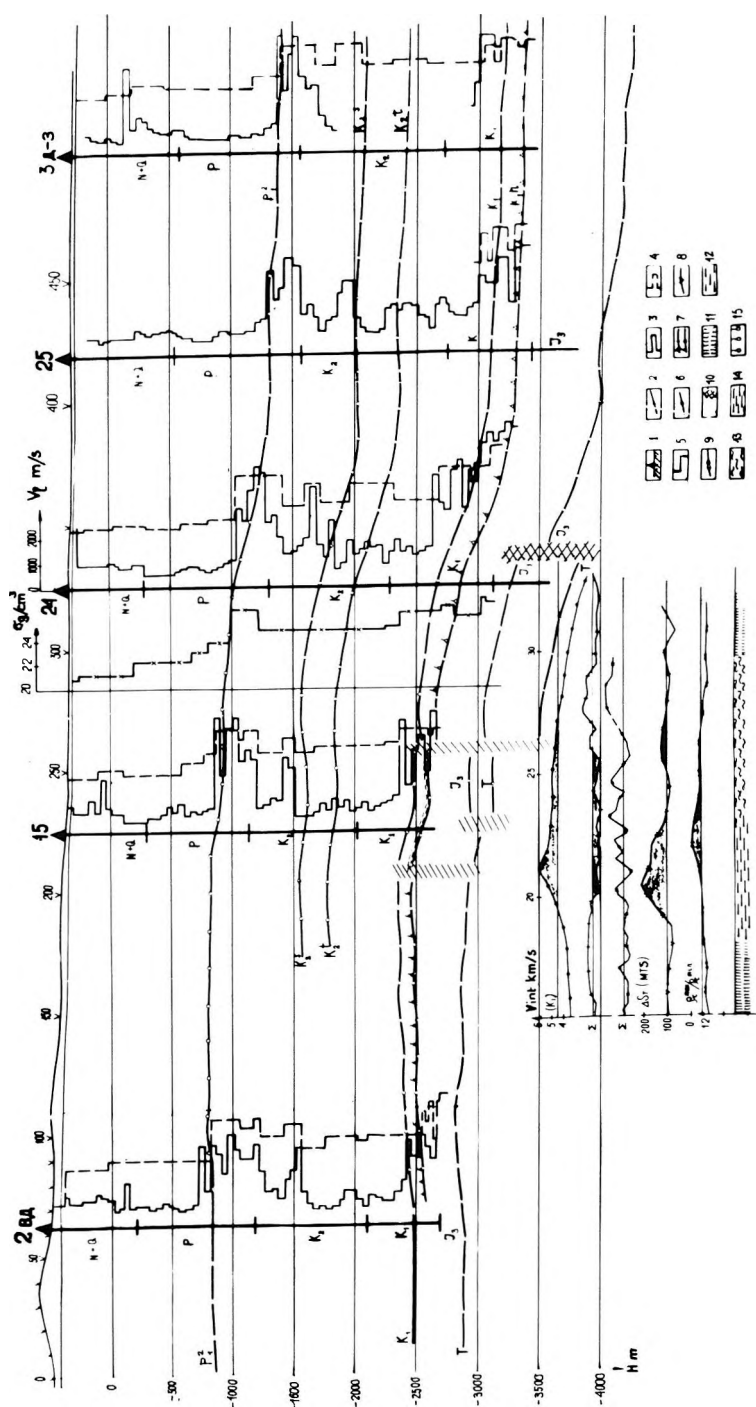


*Fig. 2.* Fragment of seismic time section (line Б—Б' in Fig. 1)

2. ábra. Az I. ára  $B - B'$  vonala mentén felvett szelvényszínt időszakosan részlete

Рис. 2. Фрагменты временного сейсмического разреза (линия Б—Б' на рис. 1).



guished with comparative certainty. Positive-to-negative transition of parameter values takes place in the vicinity of the gas—water interfaces.

The data of other geophysical methods are less informative but they supplement and refine the seismic prospecting data to a fairly high degree. MTS impedance curves, for example, have abnormal distortions within the water lens, recorded in the form of local minima indicating a lower impedance zone occurring on the section. In the field of vertical increments of apparent longitudinal conduction and in summarized longitudinal conduction the anomalous zones are identified by the maxima of these parameters. A similar maximum was recorded within the northern gas—water interfaces and outside the section contours. Judging from the transient magnetotelluric sounding data, the water lens coincides with the anomalous zone of the parameters (Fig. 3).

*Fig. 3. Curves of geophysical parameters within the water lens (line Б—Б') as compared with the seismic section and drilling results (along line А—А')*

1 — boreholes; 2 — marker horizons; 3 — resistivity; 4 — layer velocity; 5 — density; 6 — interval velocity; 7 — summarized dynamic parameter defined by standard time section (upper mark) and by corrected amplitude time sections (lower mark); 8 — increments of apparent longitudinal conduction (according to MTS); 9 —  $\varrho_t^{\max}/\varrho_t^{\min}$  curve (according to TEM); 10 — supposed tectonic dislocations (from seismic data). Local zones identified by the results of areal processing of the gravity data, showing: 11 — maximum probable presence of gas; 12 — maximum probable absence of gas; 13 — equally possible presence or absence of gas. 14 — Water lens; 15 — gas field

*3. ábra. A vizlencsét metsző vonalon (Б—Б') végzett geofizikai mérések, és az А—А' vonalon kapott fúrási adatok összehasonlítása*

1 — fúrás; 2 — vezérszint; 3 — ellenállás; 4 — rétegsebesség; 5 — sűrűség; 6 — intervallumsebesség; 7 — összegzett dinamikus paraméter, standard időszelvény alapján (felső jel) és korrigált amplitúdójú időszelvény alapján (alsó jel); 8 — a látszólagos ellenállás longitudinális növekményei (MTS-adatok). 9 —  $\varrho_t^{\max}/\varrho_t^{\min}$ -görbe (TEM-mérések alapján); 10 — feltételezett tektonikus elmozdulások (szeizmikus adatokból). A gravitációs adatok területifeldolgozása alapján azonosított lokális zónák: 11 — gáz előfordulásának maximális valószínűsége; 12 — gáz hiányának maximális valószínűsége; 13 — gáz előfordulásának és hiányának egyenlő valószínűsége. 14 — Vízlencse; 15 — gázmező

*Рис. 3. Графики геофизических параметров в пределах водяной линзы (линия Б—Б') в сопоставлении с глубинным сейсмическим разрезом и результатами глубокого бурения (по линии А—А')*

1 — глубокие скважины; 2 — опорные отражающие горизонты. Графики изменения с глубиной: 3 — электрического сопротивления; 4 — пластовой скорости; 5 — плотности. Графики геофизических параметров: 6 — интервальной скорости; 7 — суммарного динамического параметра, определенного: высший — по стандартному временному разрезу, низкий — по временному разрезу СОА; 8 — приращения кажущейся продольной проводимости (по МТЗ); 9 — график  $\varrho_t^{\max}/\varrho_t^{\min}$  (по ЗСМ); 10 — предполагаемые тектонические нарушения (по данным сейсморазведки). Локальные зоны, выделенные по результатам площадной обработки гравиметрических данных, характеризующие: 11 — высокую вероятность присутствия газа; 12 — высокую вероятность отсутствия газа; 13 — равную вероятность присутствия или отсутствия газа. 14 — Область водяной линзы; 15 — поле газовой залежи

The data of high-facility gravitation studies enables the water lens and the adjacent zone of layers dipping north in a monoclinal manner to be considered as a unit, i.e. as a transition zone characterized by small-amplitude, sign-changing and not very extensive local anomalies most often recorded within small structures with a hydrocarbon deposit. The not very extensive mosaic structural pattern of local anomalous zones, the abrupt change of signs and the strike lines of anomalies, etc. all point to the complex structure of the transition zone. Its section may contain irregularities of various sizes and different in physico-geological characteristics. This concept is also confirmed by the distribution pattern of anomalous zones identified by means of directed narrow-band reception technique. The results produced after the data of high-facility gravitation prospecting processed by different methods have made it possible to imagine that the hydrocarbon deposit is not so widely spread over the transition zone but restricted to some localities of near N—S strike.

## 5. Conclusions

The results allow the following to be stated:

- a) The most informative data for studying the water saturated lens and reservoir contours are amplitude characteristics of reflections from the pay zone boundaries and interval velocities.
- b) The data of precision gravity and electric prospecting supplement the seismic prospecting data and ensure more reliable identification of the water saturated lens, and the gas—water and water—oil interfaces.
- c) Reliable information on structural peculiarities of objects having complex tectonic pattern can only be obtained by different geophysical methods and by integration of all these methods.

**A GEOFIZIKAI KUTATÁSI ADATOK KOMPLEX ÉRTELMEZÉSE TÁROLÓ-TÍPUSÚ ANOMÁLIÁK KIMUTATÁSÁRA**

R. G. BERZIN, E. A. KOZLOV, O. A. POTAPOV, V. S. PAVLUSIN, Y. A. TARASZOV, S. S. CSAMO

A tanulmány egy Délnyugat-Türkméniában fekvő szénhidrogén-lelőhely példáján bemutatja a geofizikai módszerek komplex alkalmazásának hatékonyságát a tároló határainak kijelölésében és a benne elhelyezkedő vízlencsék lokalizálásában. Jóllehet a legtöbb információt a szeizmikus módszerek nyújtják, a precíziós gravitációs és geoelektronos módszerek hasznos kiegészítő adatokkal járulnak hozzá a geológiai inhomogenitások, a tárolókat jellemző litofácies változások meghatározásához, valamint a gáz—víz és olaj—víz határfelületek lokalizálásához.

**КОМПЛЕКСНАЯ ИНТЕРПРЕТАЦИЯ ДАННЫХ РАЗВЕДОЧНОЙ ГЕОФИЗИКИ С ЦЕЛЬЮ ВЫДЕЛЕНИЯ АНОМАЛЬНЫХ ЗОН**

Р. Г. БЕРЗИН, Е. А. КОЗЛОВ, О. А. ПОТАПОВ, В. С. ПАВЛУШИН, Ю. А. ТАРАСОВ, С. С. ЧАМО

На примере одного из месторождений углеводородов Юго-Западной Туркмении показана целесообразность комплексирования геофизических методов как для уточнения контуров залежи, так и для выявления в пределах этих контуров водяных линз. Хотя наиболее информативным является метод сейсморазведки, но при изучении сложнопостроенных объектов разведки дополнительную и часто важную чию даёт высокоточная гравиметрия и электроразведка. Комплексная интерпретация данных разведочной геофизики обеспечивает повышение надежности выявления неоднородностей геологического разреза, обнаружения зон лито-фациального замещения коллекторов, ГВК и НВК.

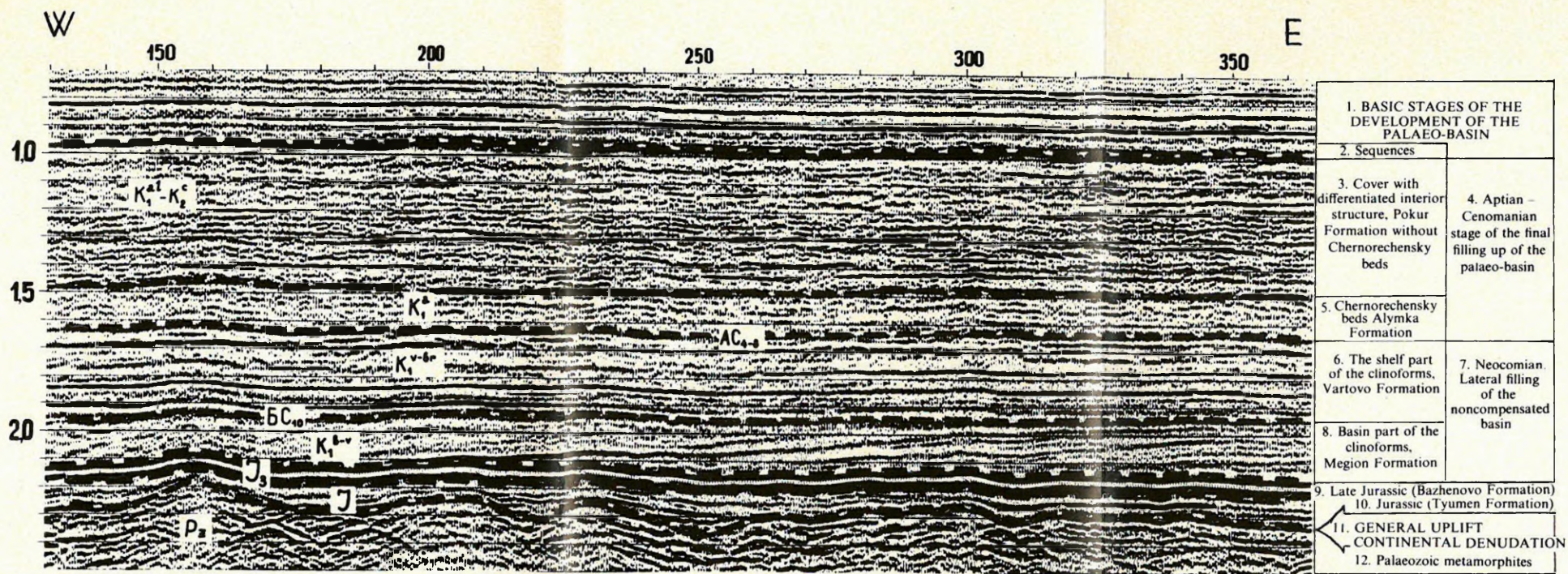


Fig. 3. Division of a seismic section of the Fedorovskaya area into seismic sequences

3. ábra. A Fedorovszkaja terület szeizmikus szelvényeinek felosztása szeizmikus rétegsorokra  
 1—A PALEO-MEĐENCE FEJLŐDÉSÉNEK SZAKASZAI; 2—rétegsorok; 3—differenciált belső szerkezetű fedő (Pokur Formáció, Csernorecsenszki rétegek nélkül); 4—a paleo-medence apti-cenomániai feltöltődése; 5—fedőréteg differenciálattal szkezettel, Csernorecsenszki rétegek, Alümka Formáció; 6—a klinoform összlet shelf-része, Vartovo Formáció; 7—nokom. A nem-kompenzált medence oldalirányú feltöltődése; 8—a klinoform összlet medence-része; 9—a zavartalan szedimentáció keső jura szakasza (Bazsenovo formáció); 10—jura, a feltöltődés kezdeti szakasza (Tyumeni Formáció); 11—ÁLTALÁNOS KIEMELKEDÉS, KONTINENTINÁLIS LEPUSZTULÁS; 12—paleozoós metamorfítok

Рис. 3. Выделение седиментационных сейсмических комплексов на временном разрезе Федоровской площади

1—ОСНОВНЫЕ ЭТАПЫ РАЗВИТИЯ ПАЛЕОБАССЕЙНА; 2—комpleксы; 3—покров с дифференцированным внутренним строением, Покурская свита без чернореченской толщи; 4—апт-сеноманский этап конечного заполнения палеобассейна; 5—покров с недифференцированным внутренним строением, чернореченская толща, альмская свита; 6—покров — шельфовая часть клиноформы, вартовская свита; 7—неокомский этап бокового заполнения некомпенсированной впадины; 8—депрессионная часть клиноформы, мигионская свита; 9—позднеюрский этап успокоения (Баженовская свита); 10—юрский этап начального заполнения (Тюменская свита); 11—ОБЩЕЕ ВОЗДЫМАНИЕ, КОНТИНЕНТАЛЬНАЯ ДЕНУДАЦИЯ; 12—палеозойский переходный этаж